NASA Technical Memorandum 83283

Development of Low-Frequency Kernel-Function Aerodynamics for Comparison With Time-Dependent Finite-Difference Methods

Samuel R. Bland

MAY 1982

NASA

NASA Technical Memorandum 83283

Development of Low-Frequency Kernel-Function Aerodynamics for Comparison With Time-Dependent Finite-Difference Methods

Samuel R. Bland
Langley Research Center
Hampton, Virginia

National Aeronautics
and Space Administration

**Scientific and Technical
Information Office**

1982

SUMMARY

Finite-difference methods for unsteady transonic flow frequently use simplified equations in which certain of the time-dependent terms are omitted from the governing equations. This paper derives kernel functions for two-dimensional subsonic flow which provide accurate solutions of the linearized potential equation with the same time-dependent terms omitted. These solutions make possible a direct evaluation of the finite-difference codes for the linear problem. Calculations with two of these low-frequency kernel functions verify the accuracy of the LTRAN2 and HYTRAN2 finite-difference codes. Comparisons of the low-frequency kernel-function results with the Possio-kernel-function solution of the complete linear equations indicate the adequacy of the HYTRAN approximation for frequencies in the range of interest for flutter calculations.

INTRODUCTION

Time-dependent finite-difference methods are receiving increased use for aeroelastic calculations in transonic flow. These methods are implemented by computer codes that solve various approximations to the time-dependent nonlinear potential equation. For example, the widely used LTRAN2 code (ref. 1) provides a solution to the two-dimensional small disturbance potential equation in which the only time-derivative term retained is the first derivative term in the differential equation. A more accurate approximation is made with the HYTRAN2 code (called LTRAN2-NRL in ref. 2), which also includes the time-derivative terms in the boundary conditions and pressure calculation. In the past, the adequacy of these approximations has been assessed by comparing results from these codes with calculations based on an analytic solution of the complete linear equations. In contrast with the finite-difference codes, these linear calculations have included the second time derivative in the differential equation.

In order to more easily assess the significance of omitting some of the time-dependent terms from the equations and to evaluate the adequacy of the finite-difference codes in solving these equations, kernel-function solutions to the simplified equations have been derived. This paper gives the derivation and compares calculations using these new kernel functions with classical results from the Possio integral equation. In addition, the accuracy of the finite-difference codes in solving the linearized simplified equations is demonstrated by comparing them with the kernel-function solutions. This comparison verifies the linear theory aspects of the code and may be used to assess the adequacy of the computational grid.

SYMBOLS

b	airfoil semichord, m
C_p	pressure coefficient
ΔC_p	lifting pressure coefficient
c_{l_α}	slope of lift coefficient

c_{m_α} slope of pitching-moment coefficient about pitch axis

$H_i^{(2)}$ Hankel function of second kind for order i

K kernel function

k reduced frequency, $b\omega/U$

M free-stream Mach number

N integral (see eq. (A23) or (A43))

P pressure term in integral equation, ΔC_p

$P_n^{(1/2,-1/2)}$ Jacobi polynomial

r scaled x-variable, $M^2k(x - \xi)/\beta^2$

s scaled y-variable, M^2ky/β^2

t dimensionless time, Ut'/b

t' time, s

U free-stream velocity, m/s

u scaled x-variable, $k(x - \xi)/\beta^2$

v scaled y-variable, ky/β^2

w dimensionless downwash, w'/U

w' downwash velocity, m/s

x dimensionless x-variable, x'/b

x' streamwise coordinate, positive downstream from midchord, m

y dimensionless y-variable, $\beta y'/b$

y' coordinate normal to free stream, m

z dimensionless mode shape, z'/b

z' airfoil mode shape, m

β $= \sqrt{1 - M^2}$

θ angle variable (see sketch B)

λ, μ, τ integration variables

ν parameter (see eq. (A10))

ξ dummy x-variable

ρ radial variable (see sketch B)

σ Fourier transform variable

ϕ dimensionless velocity potential, ϕ'/bU

ϕ' velocity potential, m^2/s

ψ dimensionless acceleration potential, $-\frac{1}{2} C_p$

ω oscillation frequency, rad/s

Subscripts:

H HYTRAN

L LTRAN

P Possio

ANALYSIS

In this section the governing differential equation, the boundary conditions, and the integral equation are presented for the classical Possio formulation and for the HYTRAN and LTRAN approximations to it. The labels HYTRAN and LTRAN are used for the kernel-function formulations which contain the same simplifications of the equations as are used in the HYTRAN2 and LTRAN2 finite-difference codes. The details of the derivation are given in the appendix.

Differential Equations and Boundary Conditions

The problem is formulated in terms of the linearized, small-disturbance, perturbation velocity potential. The differential equations and boundary conditions are derived in section 5-1 of reference 3. They are given here in terms of dimensional variables.

Complete linear equations.- In dimensional variables, indicated by primes throughout, the perturbation potential satisfies the linear differential equation

$$(1 - M^2)\phi'_{x'x'} + \phi'_{y'y'} - \frac{2M^2}{U}\phi'_{x't'} - \frac{M^2}{U^2}\phi'_{t't'} = 0 \qquad (1)$$

where M and U are free-stream Mach number and velocity, respectively. The pressure coefficient is

$$C_p = -\frac{2}{U^2}(U\phi'_{x'} + \phi'_{t'}) \qquad (2)$$

For the small perturbations treated herein, the lifting part of the problem is antisymmetric in y' and we can limit our attention to the upper-half plane. For an airfoil motion given by $z'(x',t') = 0$, the airfoil flow-tangency condition is

$$w'(x',0^+,t') = Uz'_{x'} + z'_{t'} \qquad (|x'| \leq b) \tag{3}$$

where w' is the downwash velocity on the airfoil and b is the airfoil semichord. The remaining boundary condition on the x'-axis is to require zero pressure discontinuity; that is

$$\Delta C_p(x',0,t') = C_p(x',0^-,t') - C_p(x',0^+,t') = 0 \qquad (|x'| > b) \tag{4}$$

In addition, the Kutta condition must be imposed at the trailing edge to insure a unique solution; this is enforced by requiring

$$\Delta C_p(b,0,t') = 0 \tag{5}$$

Finally, for this time-dependent problem, the Sommerfeld radiation condition requires outgoing disturbances at infinity. (See sec. 6-4 of ref. 3.)

HYTRAN equations.- The HYTRAN formulation differs from that for the linear equations in the preceding paragraph only in that the $\phi'_{t't'}$ term is omitted from the differential equation; that is, for this case, one solves

$$(1 - M^2)\phi'_{x'x'} + \phi'_{y'y'} - \frac{2M^2}{U}\phi'_{x't'} = 0 \tag{6}$$

The boundary conditions are unchanged.

LTRAN equations.- The LTRAN formulation solves the same differential equation as does the HYTRAN formulation (eq. (6)). The boundary conditions are further simplified by omitting the time-dependent terms; that is, the pressure coefficient is given by

$$C_p = -\frac{2}{U}\phi'_{x'} \tag{7}$$

and the airfoil boundary condition is

$$w'(x',0^+,t') = Uz'_{x'} \qquad (|x'| \leq b) \tag{8}$$

Integral Equations

The equations given in the preceding sections are formulated in the appendix by use of integral transforms of the acceleration potential forms of the equations. In each case, the solution is obtained from an integral equation relating the known downwash on the airfoil to the unknown lifting pressure, namely

$$w(x) = \int_{-1}^{1} P(\xi)\, K(x-\xi)\, d\xi \tag{9}$$

where nondimensional variables are now used, and w is the downwash, P is the lifting pressure, and K is the kernel function. The time dependence is removed by means of the Fourier transform and the resulting equations are for harmonic motions.

The three formulations differ only in the form of the kernel function. The forms given in this paragraph are in terms of singular integrals which must be interpreted as finite-part integrals in Hadamard's sense. Computational forms are given in the appendix. The results, expressed as integrals of the Hankel function, are as follows:

Possio kernel function:

$$K_P = -\frac{iMk}{8\beta}\, e^{-ik(x-\xi)} \int_{-\infty}^{k(x-\xi)/\beta^2} e^{i\lambda}\, H_1^{(2)}\left(M|\lambda|\right) \frac{d\lambda}{|\lambda|} \tag{10}$$

HYTRAN kernel function:

$$K_H = -\frac{iM^2k}{8\beta}\, e^{-ik(x-\xi)} \int_{-\infty}^{k(x-\xi)/\beta^2} e^{i\lambda}\, H_1^{(2)}\left(M^2|\lambda|\right) \frac{d\lambda}{|\lambda|} \tag{11}$$

LTRAN kernel function:

$$K_L = -\frac{iM^2k}{8\beta} \int_{-\infty}^{M^2k(x-\xi)/\beta^2} e^{i\lambda}\, H_1^{(2)}\left(|\lambda|\right) \frac{d\lambda}{|\lambda|} \tag{12}$$

Note that the HYTRAN kernel function may be obtained from the Possio kernel function by replacing M with M^2 in the two places M appears explicitly (not in $\beta = \sqrt{1 - M^2}$).

Finally, equation (12) demonstrates a transonic similarity law for the LTRAN formulation. One observes that K_L/β depends on a single parameter M^2k/β^2 and the variable $x - \xi$. The integral equation (9), with a slight rewriting is

$$w(x) = \int_{-1}^{1} \beta P \frac{K}{\beta} \, d\xi \tag{13}$$

so that for this equation βP also depends on the single parameter M^2k/β^2. It follows that the aerodynamic forces obey the same similarity law.

Solution of Integral Equation

Integral equation (9) was solved by a collocation procedure. The unknown pressure was approximated by a sum of 64 weighted polynomials

$$P(\xi) = \sqrt{\frac{1 - \xi}{1 + \xi}} \sum_{n=1}^{64} a_n \frac{\sin [(n - 1/2) \arccos \xi]}{\sin [(1/2) \arccos \xi]} \tag{14}$$

with unknown pressure coefficients a_n. The ratio of the sine functions is proportional to the Jacobi polynomial $P_{n-1}^{(1/2,-1/2)}$ (ref. 4, ch. 22) appropriate to the pressure weight function $\sqrt{(1 - \xi)/(1 + \xi)}$. (This weight function enforces the Kutta condition.) Equation (14) is substituted into equation (9), which leads to

$$w(x) = \sum_{n=1}^{64} a_n \int_{-1}^{1} \sqrt{\frac{1 - \xi}{1 + \xi}} \frac{\sin [(n - 1/2) \arccos \xi]}{\sin [(1/2) \arccos \xi]} K(x-\xi) \, d\xi \tag{15}$$

The integral is evaluated by the Jacobi-Gauss quadrature appropriate to the weight function for a set of 64 collocation points at which the downwash is specified. This procedure leads to a set of 64 simultaneous equations which are solved for the unknown pressure coefficients a_n. The choice of 64 collocation points gives solutions which have converged to plotting accuracy over the range of frequencies and Mach numbers considered.

RESULTS AND DISCUSSION

Calculations of aerodynamic forces for an airfoil oscillating in pitch were made with each of the three kernel functions. Comparisons among these kernel-function results are presented which show the influence of Mach number and frequency on the lift and pitching moment. A second comparison is made of calculations from the kernel functions with those from two finite-difference codes.

Kernel-Function Results

Calculations were made for a flat-plate airfoil oscillating in pitch about the quarter-chord axis at Mach numbers 0.7, 0.8, 0.9, and 0.95. The slope of the lift coefficient c_{l_α} (fig. 1) and pitching-moment coefficient c_{m_α} (fig. 2) are shown as functions of reduced frequency for each of the three kernel functions. In each figure, both the real part (in phase with the motion) and imaginary part (in quadrature with the motion) are shown.

In general, the agreement between calculations with the Possio and HYTRAN kernel functions is good, with the real parts being in better agreement than the imaginary parts and the lift being in better agreement than the pitching moment. In particular, for frequencies in the range of interest for flutter ($k < 0.2$, say), the two results are quite close together. In contrast, the LTRAN-kernel-function results differ greatly from those of the other two kernel functions even at quite low reduced frequencies. (An exception occurs in fig. 2(a) for which the curves for the real part cross at $k = 0.58$.) For example, at $M = 0.8$, the imaginary part of the LTRAN c_{l_α} (fig. 1(b)) differs by over 70 percent from the Possio value when $k = 0.1$.

Flutter calculations using each of the three kernel functions are reported in reference 5. Those calculations show the agreement between Possio- and HYTRAN-kernel-function flutter results and the disagreement between these and the LTRAN-kernel-function results that might be expected in light of the comments of the preceding paragraph.

Comparison With Finite-Difference Calculations

The finite-difference codes of references 1 and 2 have been widely used for the unsteady flow analysis of airfoils at transonic speeds. These codes provide numerical solutions to approximations of the nonlinear, small disturbance potential equation for time-dependent transonic flow. The codes, LTRAN2 and HYTRAN2, omit the same time-dependent terms from the equations as do the corresponding LTRAN and HYTRAN kernel functions, as described in the section "Analysis."

These inviscid, finite-difference codes have been evaluated in the past in two ways: by comparison with experiment or by comparison with exact linear theory. The difficulty with the former includes, among other things, the effects of viscosity and wind-tunnel walls. The problem with the latter comparison is that the equations used for the linear theory corresponded to the Possio kernel function. The development of the LTRAN and HYTRAN kernel functions herein has overcome this difficulty and has made a comparison of the finite-difference and analytical solution of the same equations possible.

An example of such a comparison between finite-difference calculations and the present analytic results is given in figure 3. The lift coefficient c_{l_α} is shown as a function of reduced frequency for an airfoil oscillating in pitch about a mid-chord axis at $M = 0.8$. The curves give the analytic results for each of the three kernel functions. The symbols show the solutions obtained from the finite-difference code of reference 2. This code permits the use of either the LTRAN2 or HYTRAN2 formulation of the problem. For the present comparisons, these codes were run with the

nonlinear terms omitted for a flat-plate airfoil to correspond with the kernel-function results. These solutions for harmonic oscillation were obtained by running the time-dependent codes through the three cycles of oscillation required for the transients to die out. There were 360 time steps per cycle, and a Fourier transform of the last cycle of oscillation was used to obtain the harmonic loads. The original 79 × 99 LTRAN2 grid was used with 33 points on the airfoil.

The agreement between the finite-difference and analytic solutions shown in figure 3 is very satisfactory. This comparison demonstrates, at least for this linear case, the accuracy of the algorithm, correctness of the coding, and adequacy of the boundary condition treatment, mesh spacing and extent, and time step size for the finite-difference methods.

CONCLUSIONS

The kernel functions for two levels of approximation to the linear equations of subsonic compressible flow have been derived. These functions were used in an integral-equation solution and compared with results from the classical Possio integral equation in order to assess the limitations of the approximations. In addition, comparisons were made with two widely used finite-difference solutions of the approximate equations.

Specific conclusions include

(1) The approximation which retains the time-derivative terms in the boundary conditions (HYTRAN-like) agrees well with the complete solution over the range of frequencies of interest in flutter calculations.

(2) The approximation which omits the time-derivative terms in the boundary conditions (LTRAN-like) is adequate only at very low frequencies.

(3) The LTRAN2 and HYTRAN2 time-dependent finite-difference codes yield accurate solutions of the corresponding approximate equations, at least for the linear case.

The analytical solutions derived herein provide objective standards for assessing attempts to enhance the efficiency of the finite-difference codes by techniques such as reducing mesh extent and increasing time step size. It is possible, of course, that the conclusions reached here may need to be modified for the nonlinear transonic-flow applications for which the finite-difference codes were developed. However, the kernel-function results can still be used to determine limits for the finite-difference parameters which may not safely be exceeded.

Langley Research Center
National Aeronautics and Space Administration
Hampton, VA 23665
April 2, 1982

APPENDIX

SOLUTION OF DIFFERENTIAL EQUATION

The derivation of the integral equation from the differential equation is presented in this appendix. The velocity-potential statement of the problem is reformulated in terms of the acceleration potential and solved by integral transform methods. The kernel functions for each of three levels of approximation are obtained and forms useful for calculation are derived.

Complete Linear Equations (Possio Kernel Function)

Kernel-function derivation.- The derivation of the Possio kernel function uses the acceleration potential to solve the linear differential equation. A derivation by superposition of singularities is given in section 6-4 of reference 3. The notation used herein is similar. The complete linear equations (eqs. (1) to (5)) are expressed in terms of the acceleration potential ψ and nondimensional coordinates. Let

$$\left.\begin{aligned} x' &= bx \\ y' &= by/\beta \\ t' &= bt/U \\ z' &= bz \\ w &= w'/U \\ \phi' &= bU\phi \end{aligned}\right\} \tag{A1}$$

and define the dimensionless acceleration potential to be

$$\phi = -\frac{1}{2} C_p = \phi_x + \phi_t \tag{A2}$$

This expression may be inverted to express the downwash in terms of the potential as

$$w(x,y,t) = \beta\phi_y = \beta \int_{-\infty}^{x} \psi_y(\lambda,y,t-x+\lambda)\, d\lambda \tag{A3}$$

which can be verified by differentiation. On the airfoil, when the antisymmetry of the pressure is taken into account,

$$P(x,t) = \Delta C_p = C_p(x,0^-,t) - C_p(x,0^+,t)$$
$$= -2C_p(x,0^+,t) \tag{A4}$$

The time dependence is removed by performing a Fourier transform on t. The result is formally equivalent to specifying simple harmonic motion by letting

$$\phi(x,y,t) = \phi(x,y)\, e^{ikt} \tag{A5}$$

and similarly for other dependent variables, where

$$k = b\omega/U \tag{A6}$$

In dealing with some of the integrals in the following analysis, it is necessary to apply analytic continuation arguments in cases for which certain integrals do not exist for real values of k. In particular, it is convenient to suppose that k has a negative imaginary part.

Collecting these results, noting that ϕ and ϕ satisfy the same differential equation, yields the following problem to be solved for $y \geq 0$:

$$\left.\begin{aligned} &\phi_{xx} + \phi_{yy} - k(M/\beta)^2(i2\phi_x - k\phi) = 0 \\ &\phi(x,0^+) = \begin{cases} \frac{1}{4} P(x) & (|x| \leq 1) \\ 0 & (|x| > 1) \end{cases} \\ &w(x,y) = \beta \int_{-\infty}^{x} e^{-ik(x-\lambda)}\, \phi_y(\lambda,y)\, d\lambda \end{aligned}\right\} \tag{A7}$$

The problem is treated by using the Fourier transform

$$\bar{\phi}(\sigma,y) = \int_{-\infty}^{\infty} e^{-i\sigma x}\, \phi(x,y)\, dx \tag{A8}$$

APPENDIX

The differential equation becomes

$$\bar{\psi}_{yy} - \nu^2\bar{\psi} = 0 \tag{A9}$$

in which

$$\nu^2 = \sigma^2 - k(M/\beta)^2(2\sigma + k) \tag{A10}$$

The solution is (the branch being chosen for which $\mathrm{Re}(\nu) > 0$)

$$\begin{aligned}\bar{\psi}(\sigma,y) &= e^{-\nu y}\,\bar{\psi}(\sigma,0^+) \\ &= \frac{1}{4}\,e^{-\nu y}\int_{-1}^{1} e^{-i\sigma\xi}\,P(\xi)\,d\xi\end{aligned} \tag{A11}$$

The Fourier inversion formula

$$\phi(\lambda,y) = \frac{1}{2\pi}\int_{-\infty}^{\infty} e^{i\lambda\sigma}\,\bar{\psi}(\sigma,y)\,d\sigma \tag{A12}$$

is used with equation (A11) and the last of equations (A7) to obtain the integral equation

$$w(x,y) = \int_{-1}^{1} P(\xi)\,K(x-\xi,y)\,d\xi \tag{A13}$$

in which the kernel function is

$$K(x-\xi,y) = \frac{\beta}{8\pi}\frac{\partial}{\partial y}\int_{-\infty}^{x} e^{-ik(x-\lambda)}\int_{-\infty}^{\infty} e^{i(\lambda-\xi)\sigma}\,e^{-\nu y}\,d\sigma\,d\lambda \tag{A14}$$

The integral-equation formulation of the original problem (eqs. (A7)) is obtained by setting $y = 0$ and using the boundary condition (see eq. (3))

$$w(x,0^+) = z_x(x) + z_t(x) \tag{A15}$$

in which $z(x)$ is the nondimensional mode shape. The inner integral in equation (A14) is evaluated as follows. Let

$$\left.\begin{aligned} \lambda &= \xi + \frac{\beta^2\bar{\lambda}}{k} \\ \sigma &= \frac{k}{\beta^2}(\bar{\sigma} + M^2) \\ x &= \xi + \frac{\beta^2 u}{k} \\ y &= \frac{\beta^2 v}{k} \end{aligned}\right\} \tag{A16}$$

Equation (A14) becomes (dropping the bars for convenience)

$$K(u,v) = \frac{k}{8\pi\beta} e^{-i\beta^2 u} \frac{\partial}{\partial v} \int_{-\infty}^{u} e^{i\lambda} \int_{-\infty}^{\infty} e^{i\lambda\sigma} e^{-v\sqrt{\sigma^2-M^2}} \, d\sigma \, d\lambda \tag{A17}$$

where now $vy = v\sqrt{\sigma^2 - M^2}$. Taking note of the parity of the inner integral yields

$$K(u,v) = \frac{k}{4\pi\beta} e^{-i\beta^2 u} \frac{\partial}{\partial v} \int_{-\infty}^{u} e^{i\lambda} \int_{0}^{\infty} e^{-v\sqrt{\sigma^2-M^2}} \cos \lambda\sigma \, d\sigma \, d\lambda \tag{A18}$$

The inner integral is a Fourier cosine transform which may be evaluated by using equation (1.4.26) of reference 6 and equations (9.6.27) and (9.6.4) of reference 4 to obtain

$$K(u,v) = \frac{ik}{8\beta} e^{-i\beta^2 u} \frac{\partial^2}{\partial v^2} \int_{-\infty}^{u} e^{i\lambda} H_0^{(2)}\left(M\sqrt{\lambda^2+v^2}\right) d\lambda \tag{A19}$$

The choice of the Hankel function of the second kind is consistent with the Sommerfeld radiation condition. For $v > 0$, the integral is well defined. To obtain the desired kernel function, one must let $v \to 0$. Using equations (9.6.1) and (9.6.27) of reference 4 yields

$$\lim_{v\to 0} \frac{\partial^2}{\partial v^2} H_0^{(2)}\left(M\sqrt{\lambda^2+v^2}\right) = -\frac{M}{|\lambda|} H_1^{(2)}(M|\lambda|) \tag{A20}$$

This result is substituted into equation (A19) to give the final expression for the Possio kernel function

$$K_p(u) = -\frac{iMk}{8\beta} e^{-i\beta^2 u} \int_{-\infty}^{u} e^{i\lambda} H_1^{(2)}(M|\lambda|) \frac{d\lambda}{|\lambda|} \tag{A21}$$

which is equation (10).

This form for the kernel function is not useful for computation in that the integrand has a second-order pole at the origin. It is possible to derive the form given in equation (6-112) of reference 3 from it, but the form in the reference also involves an integral of the Hankel function. In the following section, a form is derived which involves only a standard quadrature of an elementary function.

Computational form of kernel function.- The integral in equation (A21) does not exist for $u > 0$. This problem arose in taking the limit $v = 0$. Nevertheless, a useful computational form may be derived from it by using the integral definition of the Hankel function and deforming the path of integration in the complex plane. The formal analysis can be made rigorous by remembering that k may be assumed to have a negative imaginary part.

Equation (A21) may be rewritten as

$$K_p(u) = -i \frac{Mk}{8\beta} e^{-i\beta^2 u} N(u) \tag{A22}$$

in which

$$N(u) = \int_{-\infty}^{u} e^{i\lambda} H_1^{(2)}(M|\lambda|) \frac{d\lambda}{|\lambda|} \tag{A23}$$

It is convenient to treat positive and negative u separately by using the subscript $+$ for $u > 0$ or $-$ for $u < 0$. For $u < 0$, let $\lambda = -\bar{\lambda}$ and

$$N = N_- = \int_{|u|}^{\infty} e^{-i\lambda} H_1^{(2)}(M\lambda) \frac{d\lambda}{\lambda} \tag{A24}$$

For $u > 0$,

$$N = N_\infty + N_+ \tag{A25}$$

where

$$N_+ = -\int_{|u|}^{\infty} e^{i\lambda} H_1^{(2)}(M\lambda) \frac{d\lambda}{\lambda} \tag{A26}$$

and

$$N_\infty = \int_{-\infty}^{\infty} e^{i\lambda} H_1^{(2)}(M|\lambda|) \frac{d\lambda}{|\lambda|}$$

$$= 2 \int_0^{\infty} H_1^{(2)}(M\lambda) \cos \lambda \frac{d\lambda}{\lambda} \tag{A27}$$

The integral in equation (A27) obviously does not exist. However, remembering the source of the difficulty, one can use equation (A20) to rewrite it as

$$N_\infty = -\frac{2}{M} \lim_{v \to 0} \frac{\partial^2}{\partial v^2} \int_0^{\infty} H_0^{(2)}\left(M\sqrt{\lambda^2+v^2}\right) \cos \lambda \, d\lambda$$

$$= \frac{-i2\beta}{M} \tag{A28}$$

by equation (9.6.4) of reference 4 followed by equation (1.13.43) of reference 6. Writing equations (A24) and (A26) compactly gives

$$N_\pm = \mp \int_{|u|}^{\infty} e^{\pm i\lambda} H_1^{(2)}(M\lambda) \frac{d\lambda}{\lambda} \tag{A29}$$

From equation (9.1.6) of reference 4,

$$H_1^{(2)} = -H_{-1}^{(2)}$$

Using this result with equation (9.1.24) of reference 4, the integral becomes

$$N_\pm = \pm \frac{i2M}{\pi} \int_1^{\infty} \sqrt{\mu^2 - 1} \int_{|u|}^{\infty} e^{i(\pm 1 - M\mu)\lambda} \, d\lambda \, d\mu$$

$$= -\frac{2M}{\pi} e^{iu\cdot} \int_1^{\infty} e^{-iM|u|\mu} \frac{\sqrt{(\mu^2 - 1)}}{1 \mp M\mu} \, d\mu \tag{A30}$$

The integrand has poles at $\mu = \pm 1/M$ and branch points at $\mu = \pm 1$. The path of integration is deformed in the complex plane as indicated in sketch A.

APPENDIX

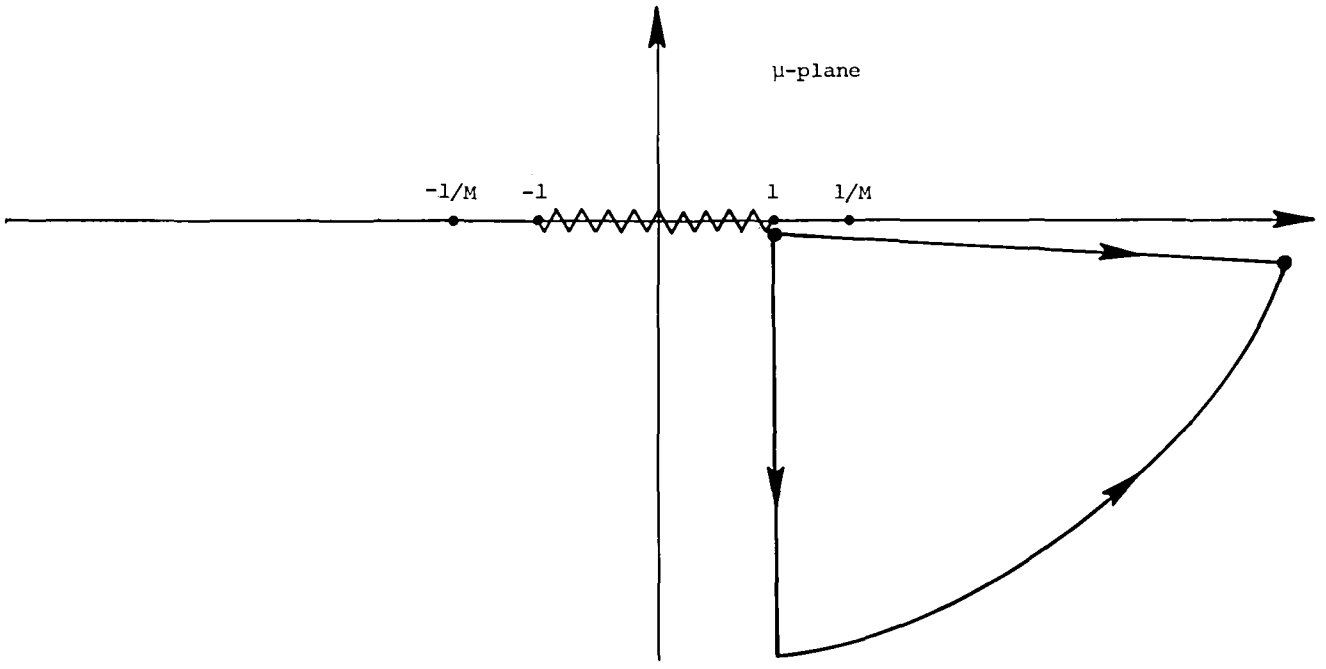

Sketch A

The integral along the arc vanishes since $\mathrm{Re}(iM|u|\mu) > 0$ there. The integral along the real axis can therefore be replaced by an integral parallel to the imaginary axis. Let $\mu = 1 - i\sigma$, then

$$\sigma = \frac{\tau}{M|u|}$$

and

$$N_{\pm} = -\frac{i2}{\pi Mu} e^{i(1\mp M)u} \int_0^{\infty} \sqrt{\tau}\, e^{-\tau} \frac{\sqrt{\tau \pm i2Mu}}{\tau - i(1 \mp M)u} d\tau \tag{A31}$$

Substituting this result and equations (A24) and (A25) into equation (A22) yields the computational form of the kernel function

$$K_p(u) = -k\, e^{-i\beta^2 u} \left[\left(1 + \frac{u}{|u|}\right) \frac{\sqrt{1 - M^2}}{8\beta} + \frac{1}{4\pi\beta u} e^{i(1\mp M)u} \int_0^{\infty} \sqrt{\tau}\, e^{-\tau} \frac{\sqrt{\tau \pm i2Mu}}{\tau - i(1 \mp M)u} d\tau \right] \tag{A32}$$

The integral may be evaluated as a Laguerre-Gauss quadrature with weight function $\sqrt{\tau}\, e^{-\tau}$.

APPENDIX

HYTRAN Equations

The HYTRAN formulation uses the same boundary conditions as the Possio formulation. However, the differential equation (eq. (1)) omits the $\phi'_{t't'}$ term for the HYTRAN formulation. In the dimensionless acceleration potential variable of this appendix, the differential equation is

$$\phi_{xx} + \phi_{yy} - i2k(M/\beta)^2\phi_x = 0 \tag{A33}$$

for the case of harmonic motion. The derivation can be carried through in a parallel fashion to that given for the Possio kernel function. One finds

$$K_H(u) = -\frac{iM^2k}{8\beta} e^{-i\beta^2 u} \int_{-\infty}^{u} e^{i\lambda} H_1^{(2)}\left(M^2|\lambda|\right) \frac{d\lambda}{|\lambda|} \tag{A34}$$

which is equation (11). As noted in the text, the HYTRAN kernel function differs from the Possio kernel function in that the HYTRAN equation has M^2 in place of the M that appears in the Possio equation.

The computational form of the HYTRAN kernel function is

$$K_H(u) = -k\, e^{-i\beta^2 u}\left[\left(1 + \frac{u}{|u|}\right)\frac{\sqrt{1 - M^4}}{8\beta} + \frac{1}{4\pi\beta u} e^{i(1\mp M^2)u}\right.$$
$$\left. \times \int_0^{\infty} \sqrt{\tau}\, e^{-\tau} \frac{\sqrt{\tau \pm i2M^2u}}{\tau - i(1 \mp M^2)u}\, d\tau\right] \tag{A35}$$

LTRAN Equations

The only time derivative in the LTRAN equations occurs in the differential equation. The differential equation is thus the same as the HYTRAN equation, but the boundary conditions and pressure coefficient use the quasi-steady expressions.

Kernel-function derivation.- The acceleration potential formulation is used again with the solution effected by use of the Fourier transform. The problem statement (eqs. (A7)) becomes

$$\left.\begin{aligned} &\phi_{xx} + \phi_{yy} - i2k(M/\beta)^2\phi_x = 0 \\ &\phi(x,0^+) = \begin{cases} \frac{1}{4}P(x) & (|x| \leq 1) \\ 0 & (|x| > 1) \end{cases} \\ &w(x,y) = \beta \int_{-\infty}^{x} \phi_y(\lambda,y)\, d\lambda \end{aligned}\right\} \tag{A36}$$

where now the acceleration potential is

$$\phi(x,y) = -\frac{1}{2} C_p = \phi_x \tag{A37}$$

The most significant difference between the HYTRAN and LTRAN formulations lies in the absence of the convective exponential term from the integral in equations (A36) (cf. eqs. (A7)).

The formal integral transform solution is carried out in a manner similar to that for the Possio formulation. The result is

$$K_L(u) = -\frac{iM^2k}{8\beta} \int_{-\infty}^{M^2u} e^{i\lambda} H_1^{(2)}(|\lambda|) \frac{d\lambda}{|\lambda|} \tag{A38}$$

which is equation (12).

Computational form of kernel function.- In contrast to the Possio and HYTRAN kernel functions, the LTRAN kernel function can be expressed in terms of Hankel functions without an integration. For this case, the analog of equation (A17) is

$$K(u,v) = \frac{k}{8\pi\beta} \frac{\partial}{\partial v} \int_{-\infty}^{u} \int_{-\infty}^{\infty} e^{i\lambda(\sigma+M^2)} e^{-v\sqrt{\sigma^2-M^4}} \, d\sigma \, d\lambda \tag{A39}$$

Let

$$\left.\begin{aligned} \lambda &= \bar{\lambda}/M^2 \\ \sigma &= M^2\bar{\sigma} \\ u &= r/M^2 \\ v &= s/M^2 \end{aligned}\right\} \tag{A40}$$

and dropping the bars, one obtains

$$K(r,s) = \frac{M^2k}{8\pi\beta} \frac{\partial}{\partial s} \int_{-\infty}^{\infty} e^{-s\sqrt{\sigma^2-1}} \int_{-\infty}^{r} e^{i(\sigma+1)\lambda} \, d\lambda \, d\sigma \tag{A41}$$

Performing the inner integration, taking the indicated derivative, and setting $s = 0$ $(y = 0)$ yields

$$K(r) = \frac{iM^2k}{8\pi\beta} e^{ir} \int_{-\infty}^{\infty} e^{ir\sigma} \sqrt{\frac{\sigma - 1}{\sigma + 1}} \, d\sigma \tag{A42}$$

APPENDIX

The branch of $\sqrt{\sigma^2 - 1}$ has been chosen for which the real part of the radical is positive as $|\mathrm{Re}(\sigma)| \to \infty$.

The integral (eq. (A42)) is evaluated by deforming the path in the complex plane. The branch chosen is defined in sketch B.

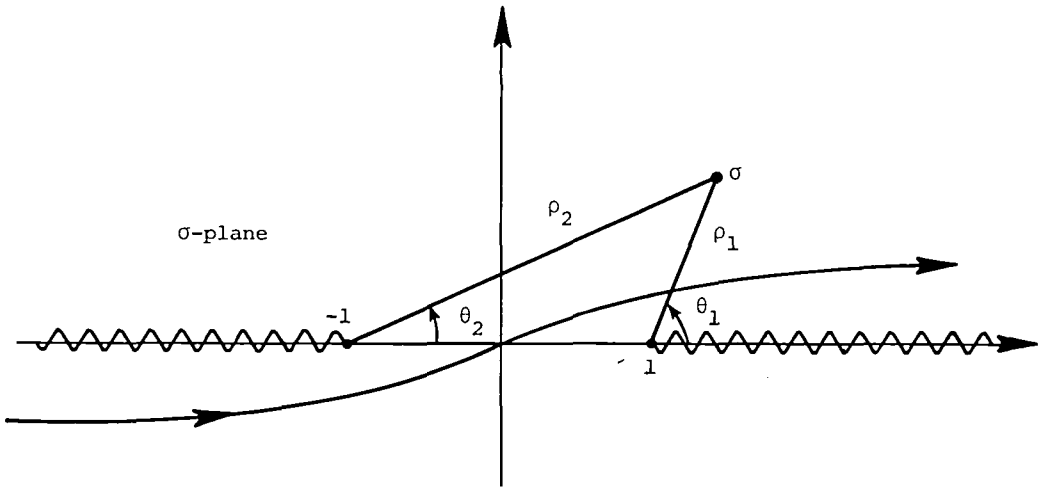

For $0 \leq \theta_1 < 2\pi$, $\sqrt{\sigma^2 - 1} = \sqrt{\rho_1 \rho_2}\, e^{i(\theta_1 + \theta_2)/2}$

For $-\pi < \theta_2 \leq \pi$, $\sqrt{\frac{\sigma - 1}{\sigma + 1}} = \sqrt{\frac{\rho_1}{\rho_2}}\, e^{i(\theta_1 - \theta_2)/2}$

Sketch B

It is convenient to treat positive and negative r separately. Let

$$N = \int_{-\infty}^{\infty} e^{ir\sigma} \sqrt{\frac{\sigma - 1}{\sigma + 1}}\, d\sigma \qquad \text{(A43)}$$

For $r > 0$,

$$\mathrm{Re}(ir\sigma) < 0$$

in the upper half-plane. The path of integration may therefore be deformed into the path shown in sketch C. The integral around the branch point vanishes since the integrand is of order $1/\sqrt{\rho_2}$ there. Below the cut,

$$\frac{\theta_1 - \theta_2}{2} = \pi$$

and above the cut,

$$\frac{\theta_1 - \theta_2}{2} = 0$$

The integrals above and below the cuts combine to give

$$N_+(r) = -2 \int_1^\infty e^{-ir\sigma} \sqrt{\frac{\sigma + 1}{\sigma - 1}}\, d\sigma \qquad \text{(A44)}$$

For $r < 0$,

$$\mathrm{Re}(ir\sigma) < 0$$

in the lower half-plane and the path of integration may be deformed as shown in sketch D. Again the integral around the branch point vanishes since the integrand is of order $\sqrt{\rho_1}$ there. Below the cut,

$$\frac{\theta_1 - \theta_2}{2} = \pi$$

and above the cut,

$$\frac{\theta_1 - \theta_2}{2} = 0$$

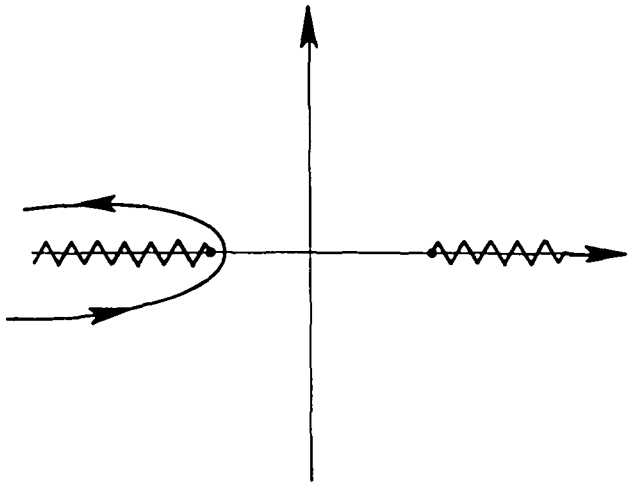

Sketch C

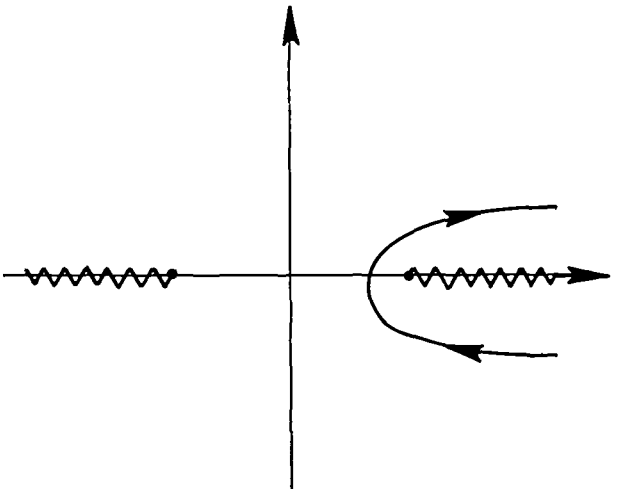

Sketch D

One obtains

$$N_-(\tau) = 2\int_1^\infty e^{ir\sigma}\sqrt{\frac{\sigma - 1}{\sigma + 1}}\,d\sigma \tag{A45}$$

The two results for $r \gtrless 0$ (eqs. (A44) and (A45)) may be written compactly as

$$\begin{aligned} N_\pm(r) &= \mp 2\int_1^\infty e^{-i|r|\sigma}\sqrt{\frac{\sigma \pm 1}{\sigma \mp 1}}\,d\sigma \\ &= -2\int_1^\infty e^{-i|r|\sigma}\,\frac{1 \pm \sigma}{\sqrt{\sigma^2 - 1}}\,d\sigma \\ &= -2\left(1 \pm i\,\frac{\partial}{\partial|r|}\right)\int_1^\infty e^{-i|r|\sigma}\,\frac{1}{\sqrt{\sigma^2 - 1}}\,d\sigma \end{aligned} \tag{A46}$$

The integral has been cast in the form of an integral representation of the Hankel function (eq. (9.1.24) of ref. 4). Thus,

$$N_\pm = i\pi\left(1 \pm i\,\frac{\partial}{\partial|r|}\right)H_0^{(2)}(|r|) \tag{A47}$$

Taking the derivative (eq. (9.1.28) of ref. 4) and substituting the result in equation (A42) yields the final expression for the LTRAN kernel function:

$$K_L(r) = -\frac{M^2k}{8\beta}\,e^{ir}\left[H_0^{(2)}(|r|) - \frac{ir}{|r|}\,H_1^{(2)}(|r|)\right] \tag{A48}$$

where

$$r = M^2u = \frac{M^2k(x - \xi)}{\beta^2}$$

This form for the LTRAN kernel function is very convenient since Bessel functions are relatively easy to compute.

REFERENCES

1. Ballhaus, W. F.; and Goorjian, P. M.: Implicit Finite-Difference Computations of Unsteady Transonic Flow About Airfoils. AIAA J., vol. 15, no. 12, Dec. 1977, pp. 1728-1735.

2. Houwink, R.; and Van der Vooren, J.: Improved Version of LTRAN2 for Unsteady Transonic Flow Computations. AIAA J., vol. 18, no. 8, Aug. 1980, pp. 1008-1010.

3. Bisplinghoff, Raymond L.; Ashley, Holt; and Halfman, Robert L.: Aeroelasticity. Addision-Wesley Pub. Co., Inc., c.1955.

4. Abramowitz, Milton; and Stegun, Irene A., eds.: Handbook of Mathematical Functions With Formulas, Graphs, and Mathematical Tables. NBS Appl. Math. Ser. 55, U.S. Dep. Commer., June 1964.

5. Edwards, John W.; Bennett, Robert M.; Whitlow, Woodrow, Jr.; and Seidel, David A.: Time-Marching Transonic Flutter Solutions Including Angle-of-Attack Effects. AIAA-82-0685, May 1982.

6. Staff of Bateman Manuscript Project, compiler: Tables of Integral Transforms. Volume I. McGraw-Hill Book Co., Inc., 1954.

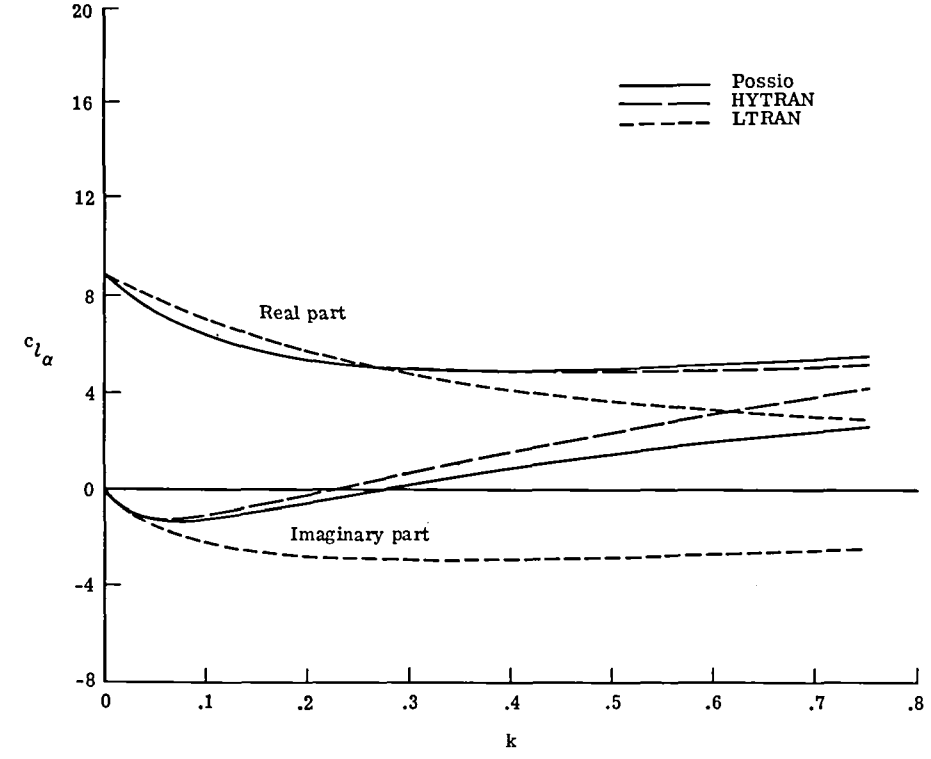

(a) M = 0.7.

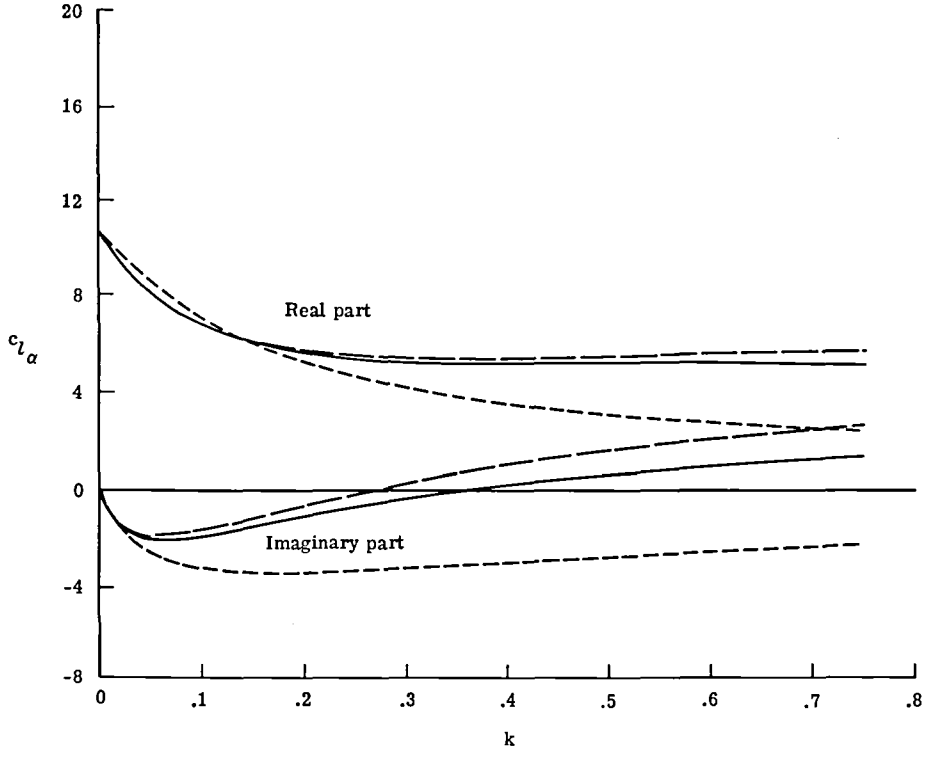

(b) M = 0.8.

Figure 1.- Comparison of lift coefficients for three methods.

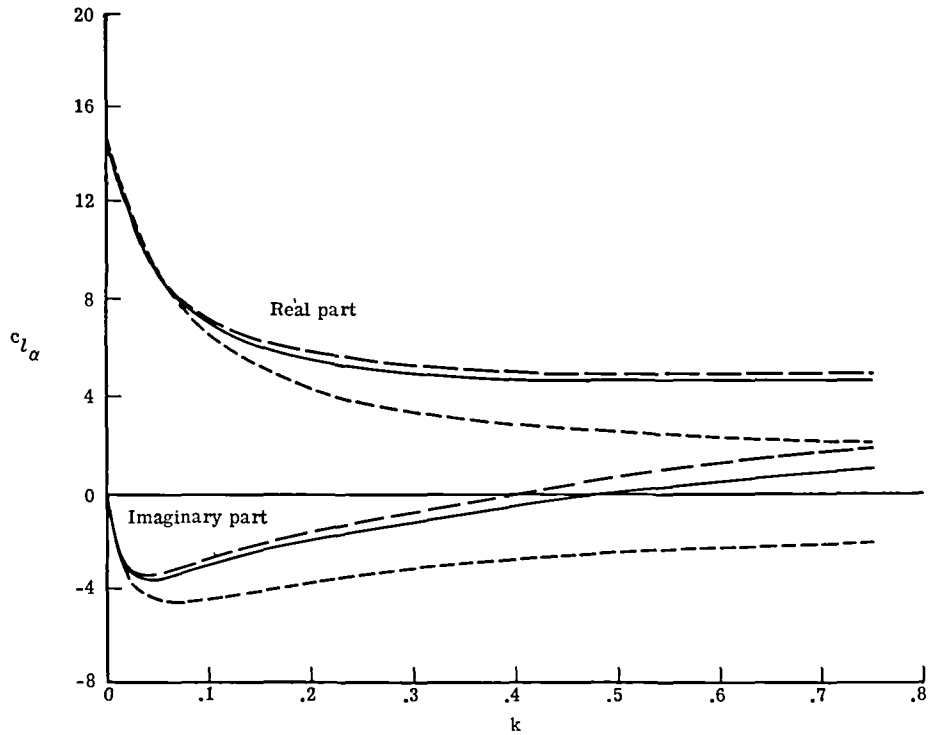

(c) M = 0.9.

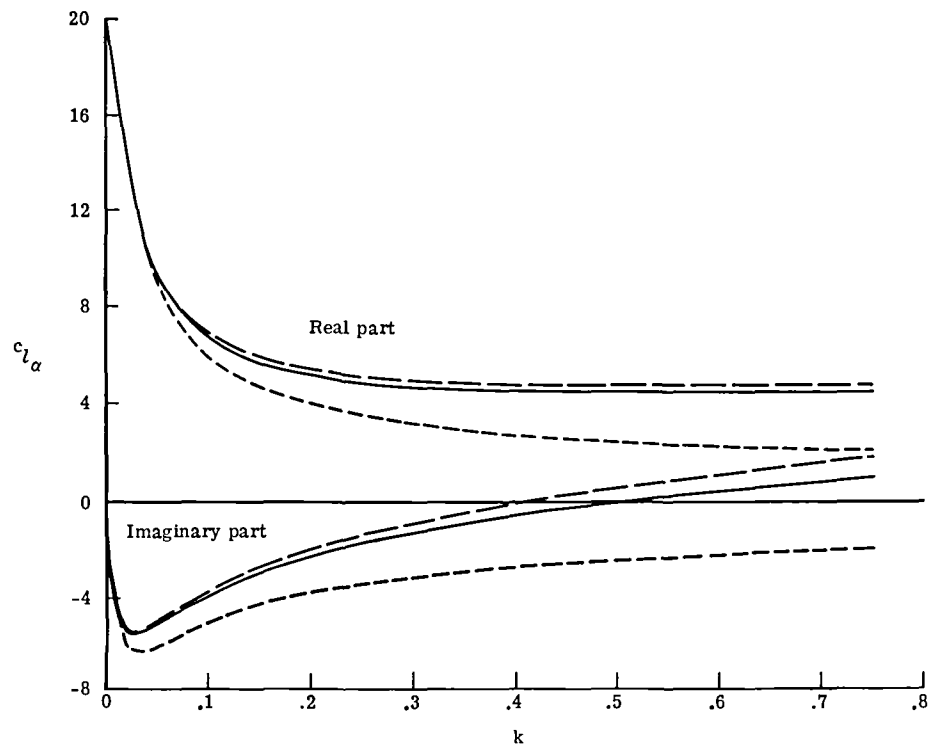

(d) M = 0.95.

Figure 1.- Concluded.

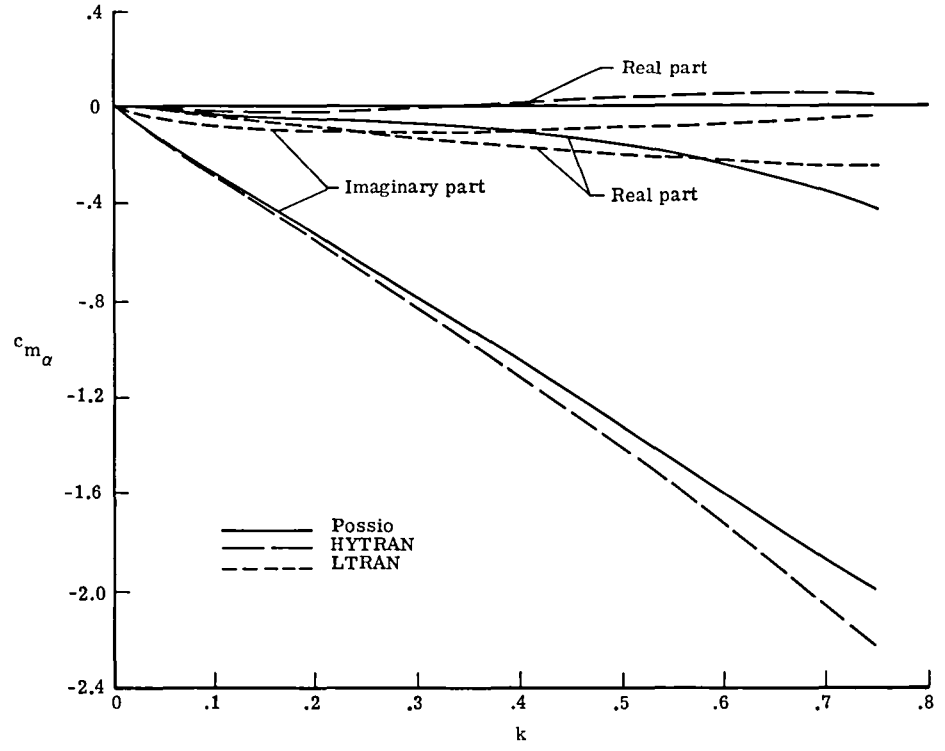

(a) M = 0.7.

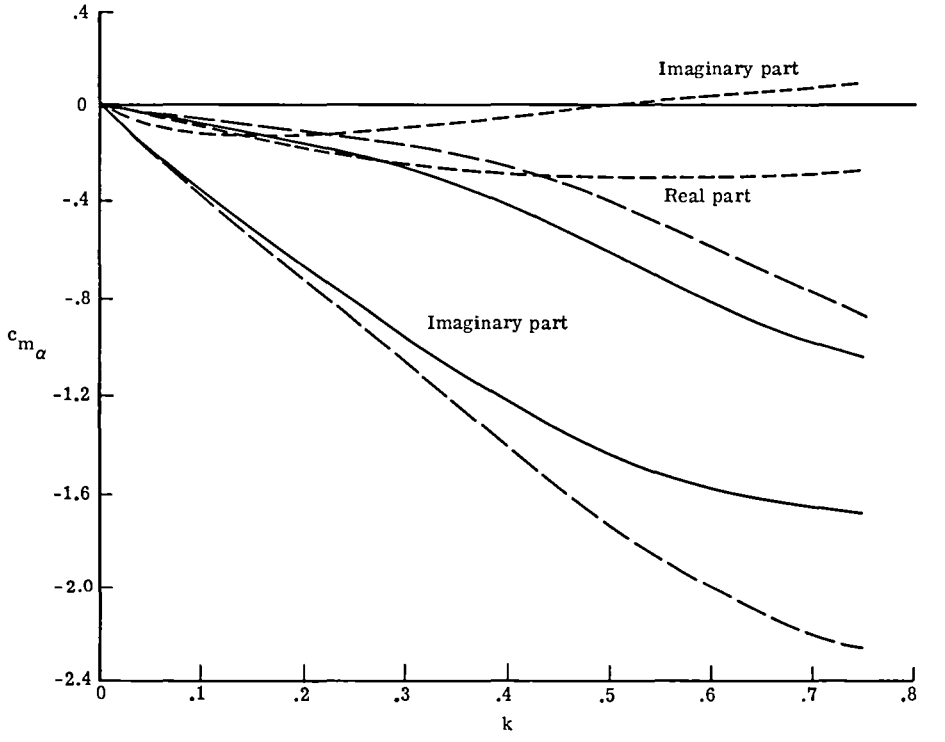

(b) M = 0.8.

Figure 2.- Comparison of pitching-moment coefficients for three methods.

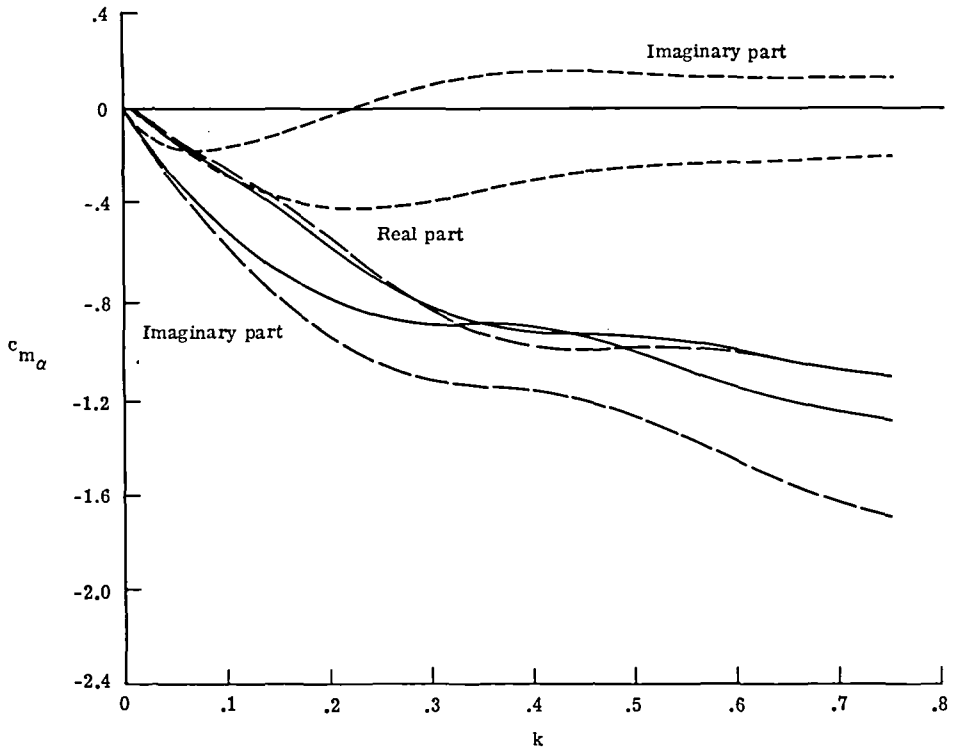

(c) M = 0.9.

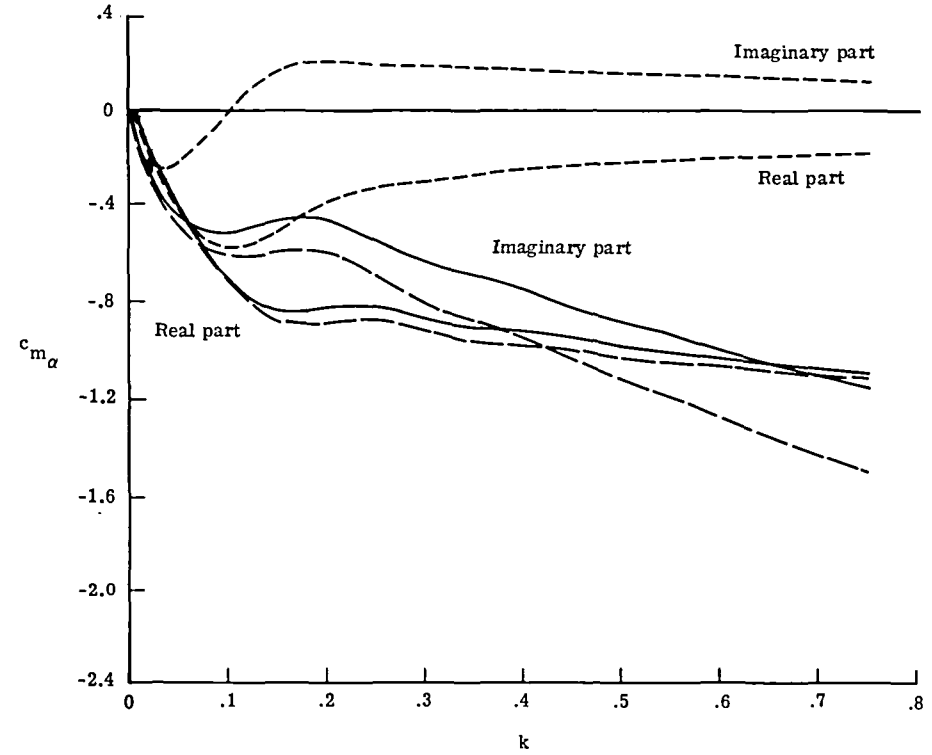

(d) M = 0.95.

Figure 2.- Concluded.

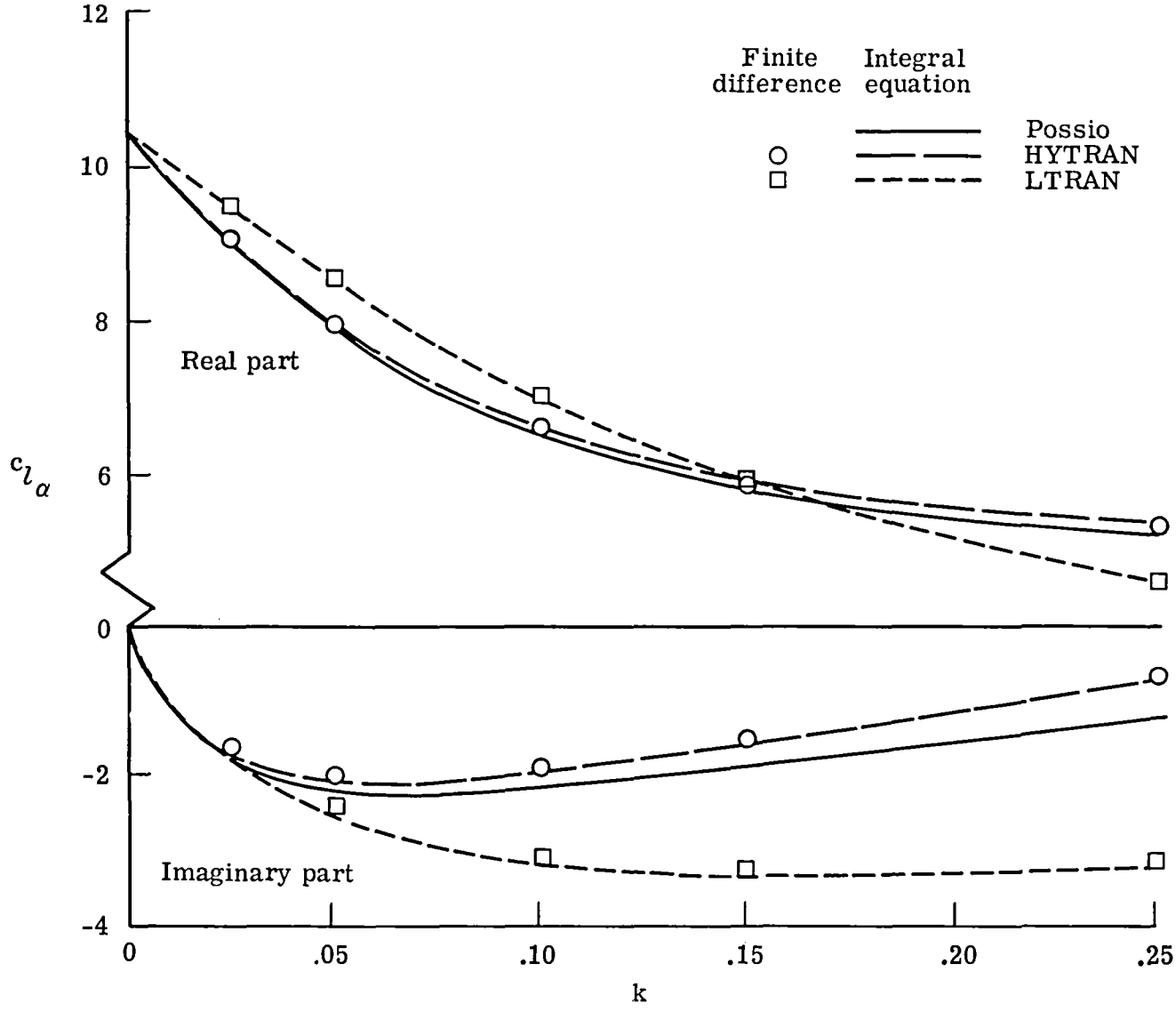

Figure 3.- Comparison of analytic and finite-difference methods at M = 0.8.

1. Report No.	2. Government Accession No.	3. Recipient's Catalog No.
NASA TM-83283		

4. Title and Subtitle	5. Report Date
DEVELOPMENT OF LOW-FREQUENCY KERNEL-FUNCTION AERODYNAMICS FOR COMPARISON WITH TIME-DEPENDENT FINITE-DIFFERENCE METHODS	May 1982
	6. Performing Organization Code 505-33-53-07
7. Author(s)	8. Performing Organization Report No.
Samuel R. Bland	L-15226
	10. Work Unit No.
9. Performing Organization Name and Address	
NASA Langley Research Center Hampton, VA 23665	11. Contract or Grant No.
	13. Type of Report and Period Covered
12. Sponsoring Agency Name and Address	Technical Memorandum
National Aeronautics and Space Administration Washington, DC 20546	14. Sponsoring Agency Code

15. Supplementary Notes

16. Abstract

Finite-difference methods for unsteady transonic flow frequently use simplified equations in which certain of the time-dependent terms are omitted from the governing equations. This paper derives kernel functions for two-dimensional subsonic flow which provide accurate solutions of the linearized potential equation with the same time-dependent terms omitted. These solutions make possible a direct evaluation of the finite-difference codes for the linear problem. Calculations with two of these low-frequency kernel functions verify the accuracy of the LTRAN2 and HYTRAN2 finite-difference codes. Comparisons of the low-frequency kernel-function results with the Possio-kernel-function solution of the complete linear equations indicate the adequacy of the HYTRAN approximation for frequencies in the range of interest for flutter calculations.

17. Key Words (Suggested by Author(s))	18. Distribution Statement
Unsteady aerodynamics Low frequency Kernel function	Unclassified - Unlimited Subject Category 02

19. Security Classif. (of this report)	20. Security Classif. (of this page)	21. No. of Pages	22. Price
Unclassified	Unclassified	27	A03

For sale by the National Technical Information Service, Springfield, Virginia 22161

NASA-Langley, 1982

National Aeronautics and
Space Administration

Washington, D.C.
20546

Official Business
Penalty for Private Use, $300

THIRD-CLASS BULK RATE

Postage and Fees Paid
National Aeronautics and
Space Administration
NASA-451

POSTMASTER: If Undeliverable (Section 158 Postal Manual) Do Not Return